PROTON-PROTON CORRELATIONS IN CENTRAL HEAVY-ION COLLISIONS AT SIS ENERGIES AND THE SPACE-TIME EXTENT OF THE EMISSION SOURCE

R. KOTTE

Forschungszentrum Rossendorf, PF 510119, D-01314 Dresden, Germany

E-mail: kotte@fz-rossendorf.de

AND THE FOPI COLLABORATION

Small-angle correlations of proton pairs produced in central collisions of ^{58}Ni+^{58}Ni at a beam energy of 1.93 A·GeV are investigated with the outer Plastic Wall/Helitron detector combination of the FOPI detector system at GSI Darmstadt. Simultaneous comparison of longitudinal and transverse correlation functions with the predictions of the Koonin-Pratt formalism allows to unravel the space-time ambiguity of the source extension. The determination of the source rest frame is found essential for the identification of this effect. For the present system, the selection of central events comprising about 8% of the total integrated cross section allows for the isolation of a compact source in momentum space which is centered around the c.m. velocity of the colliding nuclei. Taking into account the strong collective expansion of the participant zone, which introduces a reduction of the extracted source radius of more than 30%, r.m.s. radius and lifetime parameters of $R_{rms} = (4.2 \pm 1.2)$ fm and $t_{rms} = (11^{+7}_{-5})$ fm/c are extracted, respectively. In contrast, the analysis of the angle-integrated correlation function mixes the spatial and temporal size of the source and gives an upper limit $R_{rms} = (7.0 \pm 0.8)$ fm of the source radius. Additionally, recent results of correlation functions of proton pairs produced in central collisions of the systems $^{96}_{44}$Ru($^{96}_{40}$Zr)+$^{96}_{44}$Ru($^{96}_{40}$Zr) at 400, 1530 and 1690 A·MeV are presented.

1 Introduction

Two-proton correlation functions at small relative momenta can probe the space-time extent of the reaction zone created in heavy-ion reactions. This is due to the fact that the magnitude of nuclear and Coulomb final-state interactions as well as antisymmetrization effects, depend on the spatial and temporal separation of the two protons[1−12]. Usually, the correlation functions are evaluated as a function of the relative momentum $|\mathbf{q}| = \frac{1}{2}|\mathbf{p}_1 - \mathbf{p}_2|$. The attractive s-wave nuclear interaction leads to a maximum in the correlation function at $q \sim 20$ MeV/c, whereas Coulomb repulsion and antisymmetrization cause a minimum at q=0 [1]. Most analyses give only upper limits for the spatial extent of the source due to an ambiguous interplay of radius and lifetime of the source. Thus, model calculations simulating large sources with short lifetimes can give similar correlation functions as model calculations simulating small sources with long lifetimes [1,5]. However, this ambiguity may be avoided by applying cuts on the angle between the vectors of the relative momentum $\mathbf{q}$ and the total pair momentum $\mathbf{P} = \mathbf{p}_1 + \mathbf{p}_2$ [1,3,5,9].

For a source of finite lifetime τ, the phase space distribution of the emitted protons is elongated in the direction of $\mathbf{P}$ by $\langle v \rangle \tau$, where $\langle v \rangle$ is the emission velocity of the pair. For such distributions, the Pauli suppression due to the antisymmetrization of the wave functions is smaller in the elongated (longitudinal, $\mathbf{q} \| \mathbf{P}$) direction as compared to the not elongated (transverse, $\mathbf{q} \perp \mathbf{P}$) direction. Reliable impact parameter sampling is needed for the selection of well-defined sources, where certain longitudinal and transverse cuts can be applied in the source rest frame. Otherwise, the small effect of the directional dependence (about 5-10% of the height of the the correlation peak [11]) is expected to be washed out.

2 The Experiment

The experiment has been performed at the heavy-ion synchrotron SIS at GSI Darmstadt. A ^{58}Ni target of 1% interaction thickness has been irradiated by ^{58}Ni ions of $1.93A{\cdot}$GeV beam energy. The data are taken with the outer Plastic Wall/Helitron combination (which covers polar angles from 8.5 to 26.5 degrees) of the FOPI detector system [12], where the Plastic Wall delivers the velocity β and the nuclear charge Z of the particles and the Helitron allows to measure the curvature (which is a measure of the momentum over charge (p/Z)) of the particle track in the field of a large superconducting solenoid. Since the momentum resolution of the Helitron is rather moderate, this detector component serves for particle identification only. The corresponding mass is determined via $m = (p/Z)_{Hel}/(\beta\gamma/Z)_{PlaWa}$. From the velocity, which is measured with a resolution of about 1%, other kinetic quantities like the proton momenta are deduced.

3 Event Classification

Central events comprising about 8% of the total integrated cross section are selected with the online central trigger, which demands large charged particle multiplicities to be measured with the outer wall. Simulations with the IQMD model [13] predict an averaged impact parameter of 2 fm for this multiplicity cut.

In a previous investigation of central Au+Au collisions between 100 and 400 MeV per nucleon beam energy it was found that the correlation function of pairs of intermediate mass fragments (IMF) is strongly affected by the collective directed sideward flow of nuclear matter [14,15]. The directed sideflow causes an enhancement of correlations at small relative momenta. This enhancement results from mixing of differently azimuthally oriented events; it vanishes if the events are rotated into a unique reaction plane [16]. Therefore, the technique of event rotation is applied to the data in order to exclude such dynamical correlations.

4 The Correlation Function

Let $Y_{12}(\mathbf{p}_1, \mathbf{p}_2)$ be the coincidence yield of proton pairs. Then the two-particle correlation function is defined as

$$1 + R(\mathbf{p}_1, \mathbf{p}_2) = \mathcal{N} \frac{\sum_{events,pairs} Y_{12}(\mathbf{p}_1, \mathbf{p}_2)}{\sum_{events,pairs} Y_{12,mix}(\mathbf{p}_1, \mathbf{p}_2)}. \tag{1}$$

The sum runs over all events fulfilling the above mentioned global selection criteria and over all pairs satisfying certain conditions given below. Event mixing, denoted by the subscript "mix", means to take particle #1 and particle #2 from different events. We only mix events found within the same event class. $\mathcal{N}$ is a normalization factor fixed by the requirement to have the same number of true and mixed pairs. The correlation function (1) is than projected onto the relative momentum

$$q = |\mathbf{q}| = \frac{1}{2}|\mathbf{p}_1^{cm} - \mathbf{p}_2^{cm}|. \tag{2}$$

Besides the above described global event characteristics we use gate conditions on the angle α between $\mathbf{q}$ and the c.m. sum momentum of the proton pair $\mathbf{P}_{12}^{cm} = \mathbf{p}_1^{cm} + \mathbf{p}_2^{cm}$ and on the normalized pair momentum $p_{12}^o = |\mathbf{P}_{12}^{cm}|/(2 \cdot (p/A)_{proj}^{cm})$.

5 Results

Fig. 1 shows the two-proton correlation function and the relative momentum distribution of proton pairs from collisions selected with the central trigger condition. The dashed line in the lower part represents the distribution of the uncorrelated background which is produced with the event mixing technique. The statistical errors of all the correlation functions presented here are governed by those of the coincidence yield, since the mixed yield is generated with two orders of magnitude higher statistics.

Obviously, the correlation peak is governed by the contribution of very few proton pairs in the relative momentum range 10 MeV/c $< q <$ 50 MeV/c which show up above the background distribution. The corresponding yield is less than 1 per thousand. For large relative momenta the mixed yield is perfectly on

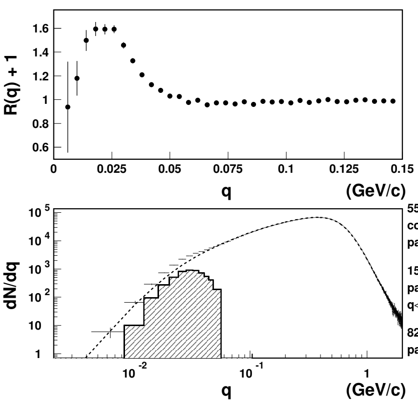

Figure 1: The experimental correlation function (upper part) and the corresponding relative momentum yield (lower part) of proton pairs from central trigger events. The dashed line represents the uncorrelated background which is constructed via event mixing. The difference of the true and mixed yield given as hatched histogram delivers the distribution of the correlated pairs.

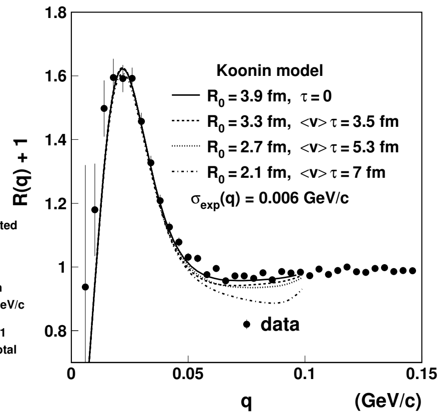

Figure 2: Correlation functions of proton pairs from Ni+Ni collisions at $1.93A$·GeV selected with the the central trigger condition (dots). The different lines are results of Koonin model simulations with different combinations of Gaussian radius and lifetime. The model results are folded with an experimental resolution function of Gaussian shape with dispersion $\sigma_{exp}(q) = 6$ MeV/c.

top of the coincidence yield. Consequently, a normalization procedure where the constant $\mathcal{N}$ in Eq. (1) is determined by the requirement that $R(q)$ vanishes for large q (cf. refs.[8,9,10,11]) would give the same correlation function.

As in previous fragment-fragment correlation analyses [14,15] an enhanced coincidence yield at very small relative angles is observed, which is due to double counting caused mainly by scattering in the scintillator strips. This surplus yield is eliminated by excluding, around a given hit, positions within a rectangular segment of $|\phi_1 - \phi_2| < 4^o$ and $|\theta_1 - \theta_2| < 2^o$. The relative-momentum distribution of the excluded proton pairs allows for a direct experimental determination of the q resolution. For these dispersions a typical value of $\sigma_{exp}(q) \simeq (6 \pm 1)$ MeV/c is estimated. In order to keep the influence of the exclusion of small angles onto the correlation function as small as possible, the same procedure is applied to the uncorrelated background. Additionally, the bias of the correlation function at very small relative momenta due to the exclusion procedure is tested with GEANT simulations using the IQMD model

[13] as event generator. It has been found that for $q > 12$ MeV/c the correlation peak, which is a measure of the source size, is almost unbiased.

In Fig. 2 the angle-integrated two-proton correlation function for central trigger events is compared with the predictions of the Koonin-Pratt formalism [1] with different combinations of the Gaussian parameters of radius R_o and lifetime (times proton pair velocity) $\langle v \rangle \tau$. The figure clearly demonstrates the space-time ambiguity of the source extension carried by the angle-integrated correlation function. The experimental correlation peak is equally well described by the model simulating either a large source ($R_{rms} = \sqrt{\frac{3}{2}} R_o = 4.8$ fm) of zero lifetime or a smaller source of finite lifetime.

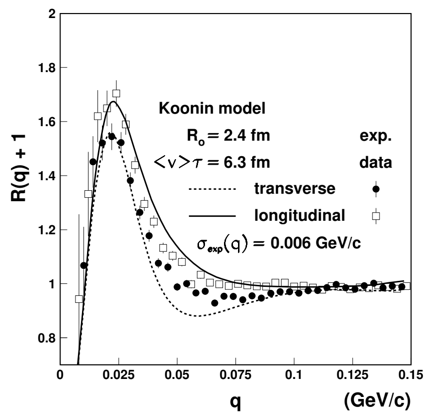

Figure 3: Transverse (dots) and longitudinal (squares) correlation functions of proton pairs from Ni+Ni collisions at $1.93A$·GeV selected with the central trigger condition. Dashed and full lines are the corresponding results of Koonin model calculations using the optimum Gaussian source parameters of radius and lifetime $R_o = 2.4$ fm and $\langle v \rangle \tau = 6.3$ fm, respectively, as delivered by the χ^2 minimum of Fig. 4.

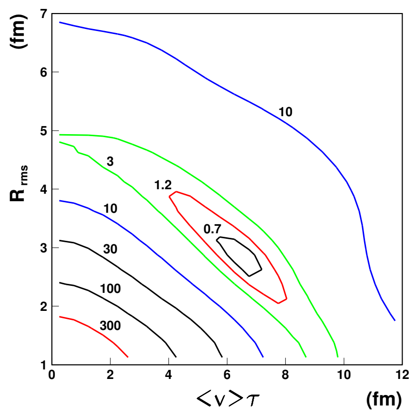

Figure 4: The distribution of χ^2 per degree of freedom as determined by simultaneously comparing measured longitudinal and transverse correlation functions (over the range 12 MeV/c $< q <$ 36 MeV/c) with the correlation functions predicted by the Koonin model. The quantity is given in dependence of the r.m.s. radius R_{rms} and Gaussian lifetime parameter $\langle v \rangle \tau$.

The space-time ambiguity of the angle-integrated correlation function can be reduced by analysing two-proton correlations with cuts on the angle $\alpha = cos^{-1}(\mathbf{P} \cdot \mathbf{q}/(Pq))$ between $\mathbf{P}$ and $\mathbf{q}$. As mentioned in Section 1, the two-proton correlation function carries a directional sensitivity due to the Pauli suppression in the non-elongated direction [1,5]. Since the pair momentum P depends on the rest frame of the source, but the relative momentum q does not, the angle α depends on the rest frame of the emitting source. Thus, a careful selection of a well-defined emission source is required. In the present analysis, we investigate correlation functions of proton pairs from central trigger events. The pair momentum is defined in the rest frame of the central source, $\mathbf{P} \equiv \mathbf{P}_{12}^{cm} = \mathbf{p}_1^{cm} + \mathbf{p}_2^{cm}$. Experimental transverse and longitudinal correlation functions are generated here by selecting proton pairs with angles $|cos(\alpha)| < 0.5$ and $|cos(\alpha)| > 0.5$, respectively. These cuts are applied both to the coincidence yield and to the uncorrelated background. The normalization constant $\mathcal{N}$ in Eq. (1) is determined individually for each α cut. The longitudinal and transverse correlation functions are presented in Fig. 3.

The wanted effect is clearly visible: We find a suppression of the transverse correlations with respect to the longitudinal ones of about 10% which is consistent with model predictions for the emission from a source of finite lifetime [1,3,5]. Koonin model calculations of longitudinal and transverse p-p correlations are performed for a wide range of Gaussian source parameters R_o and $\langle v \rangle \tau$. The results of the model are folded with the experimental resolution of $\sigma_{exp}(q) = 6$ MeV/c. In order to find the optimum set of parameters, for each set the agreement between experimental and simulated transverse and longitudinal correlation functions is tested by evaluating the χ^2 per degree of freedom in the peak region of $q = 12 - 36$ MeV/c. Fig. 4 shows, as contour plot, the distribution of this quantity as function of R_{rms} and $\langle v \rangle \tau$.

The best agreement of experimental data and model calculations is reached for Gaussian source parameters of $R_o = (2.35 \pm 0.65)$ fm and $\langle v \rangle \tau = (6.3 \pm 1.7)$ fm. The corresponding r.m.s. quantities are $R_{rms} = (2.9 \pm 0.8)$ fm and $\langle v \rangle t_{rms} = \langle v \rangle \tau / \sqrt{2} = (4.5 \pm 1.2)$ fm. The results of the Koonin model with the optimum parameter set are depicted in Fig. 3. It should be mentioned that for zero lifetime in Fig. 4 one would predict a r.m.s. radius of $R_{rms} = 4.9$ fm in nice agreement with the results of the previous analysis of the angle-integrated correlation function (cf. Fig. 2).

For the determination of the mean lifetime of the emission process one has to take into account the emission velocity of the proton pairs. For pairs of protons from central trigger events which have q values in the region of the correlation peak and which are detected within the Plastic Wall/Helitron acceptance this velocity exhibits a distribution with mean value $\langle v \rangle = 0.42$ c and dispersion $\sigma_v = 0.1$ c. Considering these quantities a r.m.s. lifetime $t_{rms} = (11^{+7}_{-5})$ fm/c can be derived.

6 Preliminary Results of Experimental p-p Correlations for the Systems $^{96}_{44}$Ru($^{96}_{40}$Zr)+$^{96}_{44}$Ru($^{96}_{40}$Zr) at 400, 1530 and 1690 A·MeV

The FOPI collaboration has continued experiments of almost complete measurements of central and semi-central heavy-ion collision. For systematic investigations of small-angle p-p correlations with respect to system size and projectile energy data sets of the following systems are available:

- ^{40}Ca+^{40}Ca at 400, 600, 800, 1000, 1500, 1930 A·MeV and Ca+Au at 1500 A·MeV (in course of calibration)
- ^{58}Ni+^{58}Ni at 1930 A·MeV (published in ref. [19])
- all projectile-target combinations of $^{96}_{44}$Ru($^{96}_{40}$Zr)+$^{96}_{44}$Ru($^{96}_{40}$Zr) at 400 and 1530 A·MeV, $^{96}_{44}$Ru+$^{96}_{44}$Ru($^{96}_{40}$Zr) at 1690 A·MeV (in course of analysis)
- Au+Au at 400, 600, 800, 1000, 1200, 1490 A·MeV (in course of calibr.)

In Fig. 5 the available angle-integrated correlation functions of proton pairs in central collision are summarized for all Ru(Zr) combinations and compared with the corresponding result of the Ni+Ni system. Obviously, the data group into three classes of correlation functions. There is one group with a low correlation peak at 1.13 for all Ru(Zr)+Ru(Zr) combinations at 400 A·MeV, another one at 1.3 for the same collision systems at the high beam energies, and a third one at 1.6 for the Ni+Ni system. The observation of the highest peak for the Ni+Ni system is quite natural since the system has the smallest participant number in the central source. Thus, one would expect a smaller source in coordinate space and consequently a higher peak than for the Ru(Zr)+Ru(Zr) system at (comparable) high beam energies. However, the strong increase of the correlation peak with increasing energy for the Ru(Zr)+Ru(Zr) systems has to be attributed to different time scales. A faster collective expansion in central nucleus-nucleus collisions at higher beam energies would reduce the influence of the time component on the angle-integrated correlation. Following the procedure described above (cf. Figs. 3, 4), the space-time ambiguity of the source extension is resolved by introducing directional cuts on the correlation function. A simultaneous fit of the transverse and longitudinal correlation functions of the Ru(Zr)+Ru(Zr) system at 1.53 A·GeV (Fig. 6) with the predictions of the Koonin-Pratt formalism delivers an optimum set of r.m.s. radius and lifetime parameters of $R_{rms} = (4.9 \pm 0.5)$ fm and $t_{rms} = (10^{+5}_{-4})$ fm/c, respectively. (Here, the proton pair velocity distribution with mean value of 0.36 c and dispersion of 0.1 c has been taken into account.)

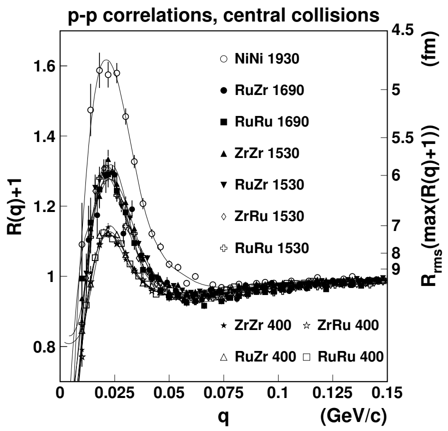

Figure 5: Angle-integrated p-p correlation functions for central events comprising an integrated cross section of about 200 - 300 mb. The projectile and target nuclei and the corresponding beam energies are indicated in the symbol list (e.g. "RuZr1530" for a 1530 A·MeV ${}^{96}_{44}$Ru projectile on a ${}^{96}_{40}$Zr target). The curves are smooth lines through the data points in order to guide the eye. The right-hand ordinate gives the r.m.s. radius $R_{rms} = \sqrt{\frac{3}{2}}R_o$ for which Koonin model simulations with zero lifetime (folded with the experimental q resolution of 6 MeV/c) would deliver the same peak height as the experimental correlation function.

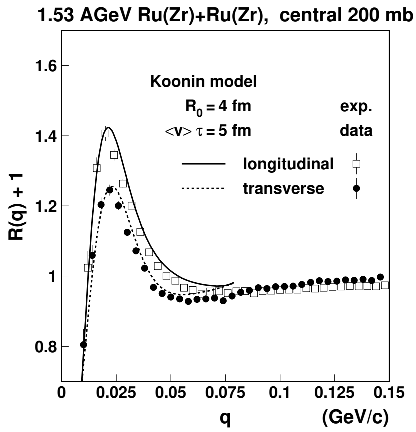

Figure 6: The angle-dependent p-p correlation functions (transverse: dots, longitudinal: squares) for central collisions of Ru(Zr)+Ru(Zr) at 1.53 A·GeV beam energy (all projectile-target combinations). Dashed and full lines are the corresponding results of Koonin model calculations using the optimum Gaussian source parameters of radius $R_o = 4$ fm and lifetime $\langle v \rangle \tau = 5$ fm as delivered by a χ^2 minimization procedure in analogy to Fig. 4. The results of the model are folded with experimental q resolution parameters of 7 MeV/c and 4 MeV/c for transverse and longitudinal correlations, respectively.

7 Discussion

Since central nucleus-nucleus collisions are characterized by a collective expansion of nuclear matter after the compression phase the question arises how does this correlation of coordinate and momentum space influence the extracted source radii. For this reason, within the Koonin model we have modified the single-proton phase space emission function [1]

$$g(\mathbf{p}, \mathbf{r}, t) \propto \exp\left(-\frac{p^2}{2mT} - \frac{r^2}{R_o^2} - \frac{t^2}{\tau^2}\right) \qquad (3)$$

by introducing a linear velocity profile which accounts for the radial expansion

$$\exp\left(-\frac{p^2}{2mT}\right) \longrightarrow \exp\left(-\frac{(\mathbf{p}-\alpha\mathbf{r})^{\mathbf{2}}}{2mT}\right). \tag{4}$$

After a lengthy but straightforward transformation one gets a relation containing a reduced radius

$$R^* = \frac{R_o}{\sqrt{1+\frac{2}{3}\frac{e_{flow}}{T}}} \tag{5}$$

instead of the true source radius R_o. Here the parameter α is connected with the (non-relativistic) radial flow energy

$$e_{flow} = \frac{\langle\alpha^2 r^2\rangle}{2m} = \frac{3}{4}\frac{\alpha^2 R_o^2}{m} = \frac{mc^2\beta_r^2}{2} \tag{6}$$

and with the radial blast velocity β_r whereas T represents the temperature.

For a quantitative estimate of the apparent reduction of the source radius we have analysed c.m. kinetic energy spectra of p, d, and t particles produced in central collisions and measured by the Plastic Wall/Helitron combination within a c.m. angular cone of $55^o < \Theta_{cm} < 70^o$. A simultaneous fit of the shape of the three spectra with the Siemens-Rasmussen formula [18] of an expanding spherical shell has been performed. From this analysis we get for the temperature and the radial blast velocity $T = (66 \pm 6)$ MeV and $\beta_r = 0.48 \pm 0.02$, respectively [19]. (For the Ru(Zr)+Ru(Zr) system at 1.53 A·GeV a fit to the p, d, t, ^3He, and α spectra within $55^o < \Theta_{cm} < 65^o$ delivers the very similar results $T = (71 \pm 5)$ MeV and $\beta_r = 0.48 \pm 0.02$.)

Taking into account these quantities the correction factor in Eq. (5) amounts to 1.45 ± 0.06 and gives a true r.m.s. radius of $R_{rms} = (4.2 \pm 1.2)$ fm. The corresponding sharp sphere radius $R_{ss} = \sqrt{5/3}R_{rms}$ allows to determine the breakup volume $V = A/\rho = 4\pi R_{ss}^3/3 = 670$ fm^3 of the source. For an estimated participant multiplicity of the central source of $A = 80$ this volume gives a breakup density of $\rho = 0.70\rho_o$. In contrast, the radius which is deduced from the angle-integrated correlation function after correcting for collective expansion amounts to $R_{rms} = (7.0 \pm 0.8)$ fm. It would give a 4.5 times larger volume than the value delivered by the correlation function with directional cuts and a correspondingly smaller breakup density of $\rho = 0.15\rho_o$.

The estimated characteristic source emission time of is the shortest one determined with the method of directional cuts on the two-proton correlation function known so far. It does well compare with predictions of calculations we have performed with the BUU transport model [6,17] for central (b=2 fm) Ni+Ni collisions at 2 A·GeV. The simulation delivers a spread ($\pm 1\sigma$) of about

10-15 fm/c for the distribution of the time instants when the nucleons undergo the last collision. Furthermore, the BUU model predicts about 3 fm/c for the time from the begin of the density increase until a maximum value of $\rho \simeq 1.8\rho_o$ is reached followed by a time of about 10 fm/c for the expansion to a density of $\rho \simeq \rho_o/4$. Thus, proton pairs contributing to the peak in the correlation function are supposed to be emitted over almost the whole radial expansion time (or even over the whole reaction time). It is certainly appropriate to assume that - in the 1-2 A·GeV energy region - proton emission is not governed by sequential decay chains but by a sudden explosion/expansion process. Dealing with such short time scales the notation "lifetime" almost looses its meaning.

8 Acknowledgement

This work was supported by the German BMBF under contract No. 06DR666.

References

1. S.E. Koonin, *Phys. Lett.* B **70**, 43 (1977).
2. S. Pratt, *Phys. Rev. Lett.* **53**, 1219 (1984).
3. S. Pratt and M.B. Tsang, *Phys. Rev.* C **36**, 2390 (1987).
4. W.G. Gong *et al.*, *Phys. Rev. Lett.* **65**, 2114 (1990).
5. W.G. Gong et al., *Phys. Rev.* C **43**, 781 (1991).
6. W. Bauer, C.K. Gelbke and S. Pratt, *Ann. Rev. Nucl. Part. Sci.* **42**, 77, (1992); W. Bauer, *Nucl. Phys.* A **545**, 369c (1992).
7. G.J. Kunde *et al.*, *Phys. Rev. Lett.* **70**, 2545 (1993).
8. M.A. Lisa *et al.*, *Phys. Rev. Lett.* **70**, 3709 (1993).
9. M.A. Lisa *et al.*, *Phys. Rev. Lett.* **71**, 2863 (1993).
10. M.A. Lisa *et al.*, *Phys. Rev.* C **49**, 2788 (1994).
11. D.O. Handzy *et al.*, *Phys. Rev.* C **50**, 858 (1994).
12. A. Gobbi *et al.* (FOPI collaboration), *Nucl. Instrum. Methods* A **324**, 156 (1993), J. Ritman, *Nucl. Phys.* (Proc. Suppl.) B **44**, 708 (1995).
13. S.A. Bass, C. Hartnack, H. Stöcker and W. Greiner, *Phys. Rev.* C **51**, 3343 (1995).
14. B. Kämpfer et al. (FOPI collaboration), *Phys. Rev.* C **48**, R955 (1993).
15. R. Kotte *et al.* (FOPI collaboration), *Phys. Rev.* C **51**, 2686 (1995).
16. P. Danielewicz and G. Odyniec, *Phys. Lett.* B **157**, 146 (1985).
17. Gy. Wolf, W. Cassing, U. Mosel, *Nucl. Phys.* A **552**, 549 (1993), *Phys. Lett.* B **271**, 43 (1991).
18. P.J. Siemens and J.O. Rasmussen, *Phys. Rev. Lett.* **42**, 880 (1979).
19. R. Kotte *et al.* (FOPI collaboration), *Z. Phys.* A **359**, 47 (1997).